A Fixed Tuned SIS Receiver for the 450 GHz Frequency Band

R. Blundell, C.-Y. E. Tong, J. W. Barrett, J. Kawamura,
R. L. Leombruno, S. Paine, D. C. Papa and X. Zhang
Harvard-Smithsonian Center for Astrophysics,
60, Garden Street, Cambridge, MA 02138, USA

J. A. Stern, H. G. LeDuc and B. Bumble
Center for Space Microelectronics Technology,
Jet Propulsion Laboratory,
California Institute of Technology,
Pasadena, CA 91109, USA

Abstract

We report on the development of a heterodyne receiver designed to cover the frequency range 400 - 500 GHz. This receiver incorporates mixer technology used in a wide band, fixed-tuned SIS receiver developed for the Submillimeter Array of the Smithsonian Astrophysical Observatory. The mixer employs a Nb SIS tunnel junction that has a current density of about 7.5 kA/cm^2 and is about 0.6 μm^2 in area. On-chip tuning is provided by a short inductor section followed by a microstrip transformer. Double sideband receiver noise temperatures, determined from experimental Y-factor measurements, are about 100 K across the majority of the desired operating frequency band. A single-sideband mixer, for operation at 460 and 490 GHz, has also been tested in the same receiver set-up. In this case, the receiver noise is about twice the double-sideband value.

I. Introduction

The Submillimeter Array (SMA), a six-element interferometer presently under construction by the Smithsonian Astrophysical Observatory, is designed to operate in the major atmospheric windows from below 200 GHz to above 900 GHz. In Figure 1 we show a plot of atmospheric transmission, typical of a high altitude site selected for submillimeter wavelength radioastronomy [1]. Also shown in the Figure are the rotational transitions of the CO molecule and the fine structure transitions of the CI atom, both of considerable astrophysical interest. Heterodyne receiver development in this wavelength range has generally taken place around 115, 230, and 345 GHz.

More recently a good deal of attention has been focussed on developing receivers for higher frequency operation [2,3,4,5]. Referring to Figure 1, the frequency band 380 - 520 GHz is discontinuous for reasonable atmospheric transmission and contains two particularly interesting spectral lines, CO ($J = 4 \rightarrow 3$) and CI ($2P^2 = {}^3P_1 \rightarrow {}^3P_0$) at 461.0408 GHz and 492.1607 GHz, respectively. While it is generally desirable for a radioastronomy receiver to cover as wide a frequency range as possible, it is essential that high efficiency operation at these frequencies be provided. Furthermore, single side band (SSB) receiver operation may offer some advantages over double side band (DSB) operation, both in terms of reducing excess atmospheric noise and the strength of unwanted spectral lines from the image sideband.

II. Mixer design

The mixer block, shown schematically in Figure 2, is made in two pieces: a corrugated horn feed, and a shorted section of reduced-height wavegude. The fused quartz substrate carrying the SIS tunnel junction is sandwiched between the two pieces in a suspended configuration. The suspended stripline circuit containing the SIS tunnel junction and low-pass filter structures for IF output and dc bias faces the corrugated horn feed.

The waveguide dimensions, shown in Figure 2, were determined by simply scaling those of an existing lower frequency mixer [6]. The length of the shorted section of waveguide was determined experimentally to be 0.16 mm for wideband DSB operation and 4.43 mm for SSB operation at 461 and 492 GHz. The dimensions of the suspended stripline filter, shown in Figure 3a, were also determined by simple scaling from the lower frequency unit.

The SIS tunnel junctions used in this work were fabricated using standard Nb trilayer technology developed at the Jet Propulsion Laboratory. In order to achieve the required junction size, ~ 0.7 μm^2, e-beam lithography was used [7]. For wideband operation a thin film microstrip matching network was inserted between the center of the suspended stripline filter and the SIS tunnel junction. This consists of a two-section impedance transformer followed by a short inductive line, and is shown in Figure 3a. Shown in Figure 3b is the calculated match between the 35 Ω impedance presented by the waveguide circuit and an SIS junction with nominal characteristics (R_N ~ 22 Ω, A ~ 0.7 μm^2, J_c ~ 10 $kAcm^{-2}$). From the Figure, a reasonably good match, better than - 12 dB, is obtained over 120 GHz bandwidth.

III. Receiver noise measurements

In all receiver noise measurements, the mixer was cooled in a liquid helium filled cryostat equipped with a liquid nitrogen cooled radiation shield. Signal input to

the mixer was via a 0.5 mm thick room-temperature Teflon vacuum window and a 1.2 mm thick Zitex film, cooled by the radiation shield, that acted as an infrared block [8]. A Teflon lens, cooled to 4.2 K, provided additional infrared filtering. Local oscillator (LO) power was provided by a Gunn oscillator and solid-state frequency multipliers, and was coupled to the receiver via either a Martin-Puplett interferometer or a simple wire grid polarizer. The intermediate frequency (IF) was 5 GHz, and the IF bandwidth, either 1 or 2.5 GHz, was selected using filters external to the cryostat. In all cases, the receiver noise was calculated from Y-factor measurements using room-temperature and liquid nitrogen cooled loads at 295 K and 77 K respectively, and no corrections were made for losses in front of the receiver.

IV. Double sideband receiver performance

In Figure 4 we show the receiver noise temperature, measured over a 2.5 GHz instantaneous bandwidth, for three different SIS junctions cooled to 4.2 K in the same mixer block. In each case the integrated microstrip tuner was identical, but the junction area and normal resistance, were varied from 0.65 to 0.5 μm^2 and 40 to 50 Ω, respectively. A Martin-Puplett interferometer was used to couple LO and signal to the receiver. From the Figure, the receiver noise is approximately 150 K over about 100 GHz bandwidth and the region of low receiver noise extends to higher frequencies as the junction area is reduced. Recalling that the nominal mixer design calls for an SIS junction with A ~ 0.65 μm^2 and R_N ~ 22 Ω, these results are encouraging.

In Figure 5, the receiver noise is plotted, for two IF bandwidths, as a function of LO frequency from about 350 to 500 GHz. For the 2.5 GHz IF bandwidth the receiver noise is approximately 130 K from about 350 to 500 GHz. The receiver noise is about 20 K lower for the reduced IF bandwidth (1 GHz). This reduction is due to a small reduction in IF amplifier noise and a reduction in input noise from the Martin-Puplett interferometer used to combine signal and LO. In Figure 6 we display current-voltage and IF response curves, measured at selected LO frequencies, for the same receiver configuration with an SIS junction with improved characteristics. At each frequency, the Josephson currents were easily suppressed by the application of a small magnetic field.

V. Single sideband receiver performance

In radioastronomy, particularly for single-dish spectral line observations, SSB receiver operation is often preferred. This is usually achieved through mechanical means: by tuning an SSB filter placed at the receiver input or by detuning the mixer backshort. We have built a fixed tuned SSB receiver for observing the spectral lines CO ($J = 4 \rightarrow 3$) and CI ($2P^2 = {}^3P_1 \rightarrow {}^3P_0$) (at 461.0408 GHz and 492.1607 GHz, respectively) using the latter approach. In this case the length of the shorted section of waveguide that acts as a fixed backshort tuner was calculated to be 4.42 mm, and

experimentally determined to be 4.43 mm. Figure 7a shows the raw interferogram of the SSB receiver when coupled to a Fourier Transform Spectrometer (FTS) designed for use in the 200 - 2000 GHz frequency range. The Fourier transform of this, giving the receiver response as a function of input frequency, is shown in Figure 7b. Clearly the receiver responds well to signals at 461 and 492 GHz and offers reduced response to 471 and 502 GHz, the corresponding image frequencies for lower sideband operation for our receiver IF of 5 GHz.

We have measured the lower sideband to upper sideband gain ratio G_{LSB}/G_{USB} of this receiver, over the frequency range 450 to 500 GHz, using a Martin-Puplett interferometer as an SSB filter. This is a laborious process, as each data point requires tuning of the receiver LO, and calibration and tuning of the SSB filter. The results of these measurements are given in Figure 8. Also shown in the Figure are the sideband gain ratios calculated directly from the receiver's FTS response shown in Figure 7b. Clearly there is excellent agreement between the measured data and that calculated from the FTS response. Referring to Figure 8, the sideband gain ratio $G_{LSB}/G_{USB} \sim 7$ indicates that LSB operation is preferred at LO frequencies of 466 and 497 GHz.

In order to compare SSB and DSB receiver performance, we have determined the receiver noise from Y-factor measurements made using the same SIS junction in the two receiver configurations. A wire grid polarizer was used to combine LO and signal at the receiver input. Figure 9 shows the receiver noise data obtained from measurements over a 1 GHz IF bandwidth. From the Figure, the SSB receiver noise is approximately twice that of the DSB receiver for LO frequencies of 466 and 497 GHz. For a perfectly transparent atmosphere, spectral line observations of CO ($J = 4 \rightarrow 3$) and CI ($2P^2 = {}^3P_1 \rightarrow {}^3P_0$) made with either receiver offer approximately equal sensitivity. However, the SSB receiver has the advantage of reducing the intensity of spectral lines falling in the image sidebands. For an atmosphere with significant attenuation in the image sidebands, the SSB receiver also offers an improvement in sensitivity over the DSB equivalent.

VI. Summary

We have developed a fixed-tuned SIS receiver for the frequency range 350 to 500 GHz. This receiver combines high sensitivity with wide IF bandwidth. A single sideband version of this receiver offers improved performance for spectral line observations of CO ($J = 4 \rightarrow 3$) and CI ($2P^2 = {}^3P_1 \rightarrow {}^3P_0$) at 461 GHz and 492 GHz respectively.

Acknowledgement

We thank M. J. Smith for his superior technical assistance in developing the mixers used in this work.

References.

[1] R. N. Martin, P. A. Strittmatter, J. H. Black, W. F. Hoffman, C. J. Hogan, C. J. Lada, and W. L. Peters, in: *"A proposal to the National Science Foundation for partial funding of the Submillimeter Telescope,"* University of Arizona, Steward Observatory, 1989.

[2] R. Blundell, and C.-Y. E. Tong, "Submillimeter receivers for radioastronomy," *Proc. IEEE,* vol. 80, pp. 1702-1720, 1992.

[3] J. W. Kooi, C. K. Walker, H. G. LeDuc, P. L. Schaffer, and T. G. Phillips, " A low noise 565 - 735 GHz SIS waveguide receiver," in: *Proc. 5th Int. Symp. Space Terahertz Tech.*, Ann Arbor, MI, pp. 126-141, 1994.

[4] Zmuidzinas, H. G. LeDuc, J. A. Stren, and S. R. Cypher, "Two junction tuning circuits for submillimeter SIS mixers, "*IEEE Trans. Microwave Theory Tech.*, vol. MTT-42, pp. 698-706, 1994.

[5] G. de Lange, J. J. Kuipers, T. M. Klapwijk, R. A. Panhuyzen, H. van de Stadt, and M. W. M. de Graauw, "Superconducting resonator circuits at frequencies above the gap frequency," *J. App. Phys.*, vol. 77, pp. 1795-1804, 1995.

[6] R. Blundell, C.-Y. E. Tong, D. C. Papa, R. L. Leombruno, X. Zhang, S. Paine, J. A. Stern, H. G. LeDuc and B. Bumble, "A Wideband Fixed-Tuned SIS Receiver for 200 GHz Operation," in: *Proc. 5th Int. Symp. Space Terahertz Tech.*, Ann Arbor, MI, pp. 27-37, 1994.

[7] H. G. LeDuc, B. Bumble, S. R. Cypher, A. J. Judas, and J. A. Stern, "Submicron area Nb/AlOx/Nb tunnel junctions for submillimeter mixer applications," in: *Proc. 3rd Int. Symp. Space Terahertz Tech.*, Ann Arbor, MI, pp. 408-418, 1992.

[8] Zitex A, a product of Norton Performance Plastics, Wayne, NJ.

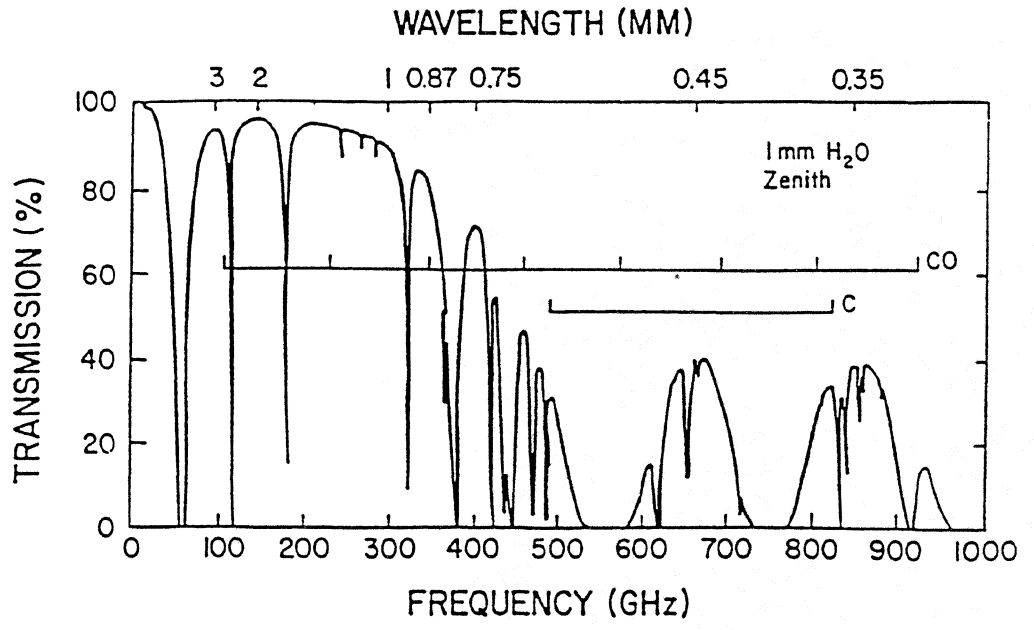

Figure 1: Atmospheric transmission at millimeter and submillimeter wavelengths from the altitude of Mt. Graham (Arizona, USA) for 1mm precipitable water along the line of sight.

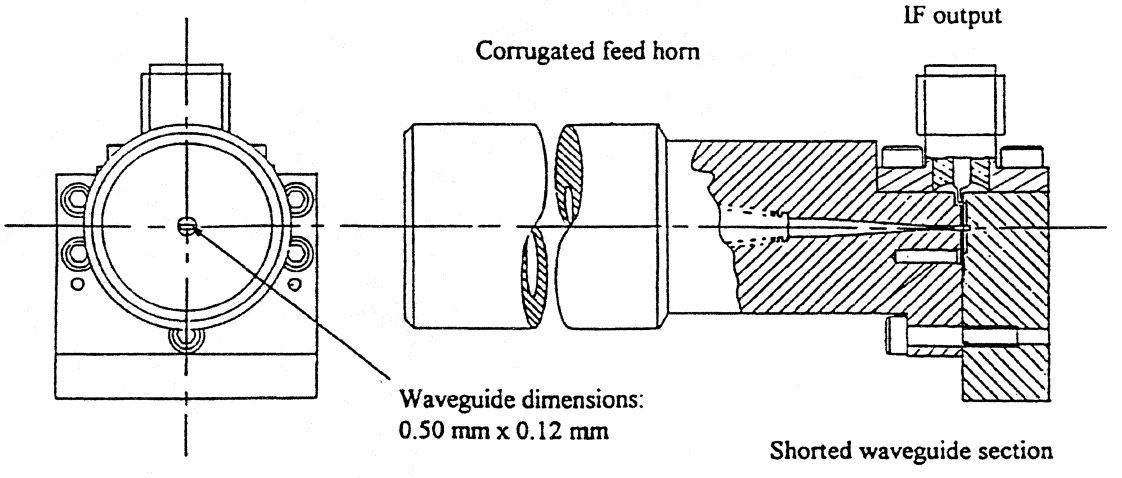

Figure 2: Mixer block detail showing the corrugated horn feed and the shorted section of reduced-height waveguide.

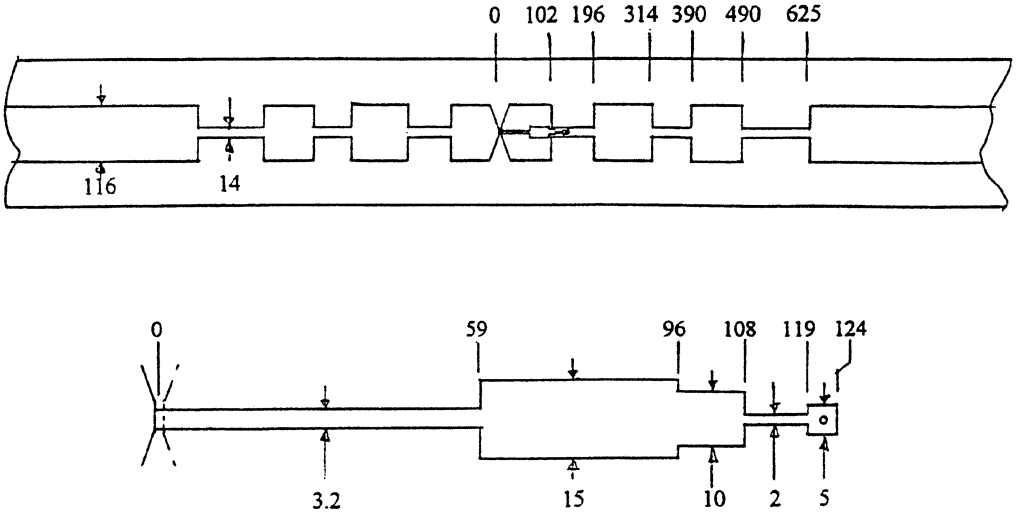

Figure 3a: Layout of the suspended stripline filter and the thin film microstripline matching network showing the SIS junction, the short inductive line and the two-section impedance transformer (dimensions in microns).

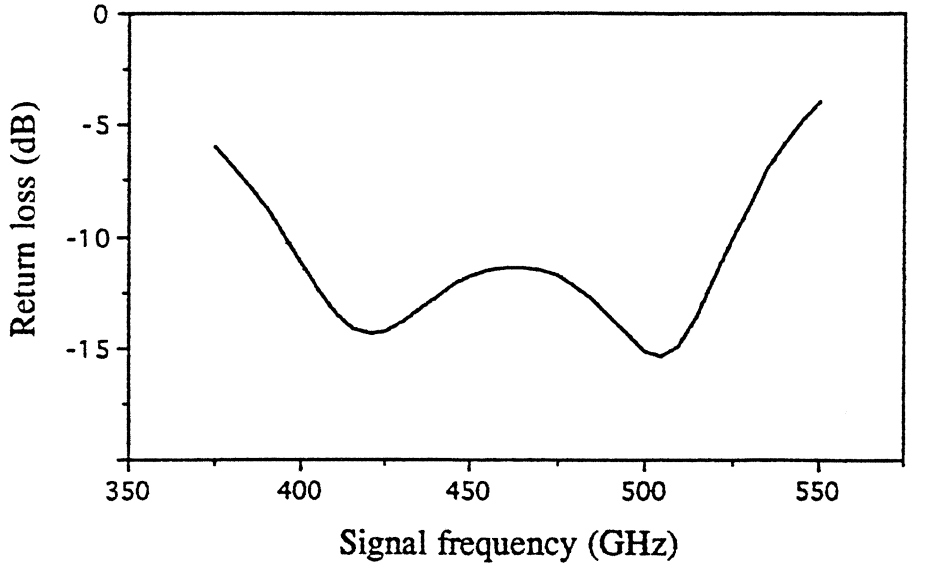

Figure 3b: Calculated match between the SIS junction and waveguide embedding circuit.

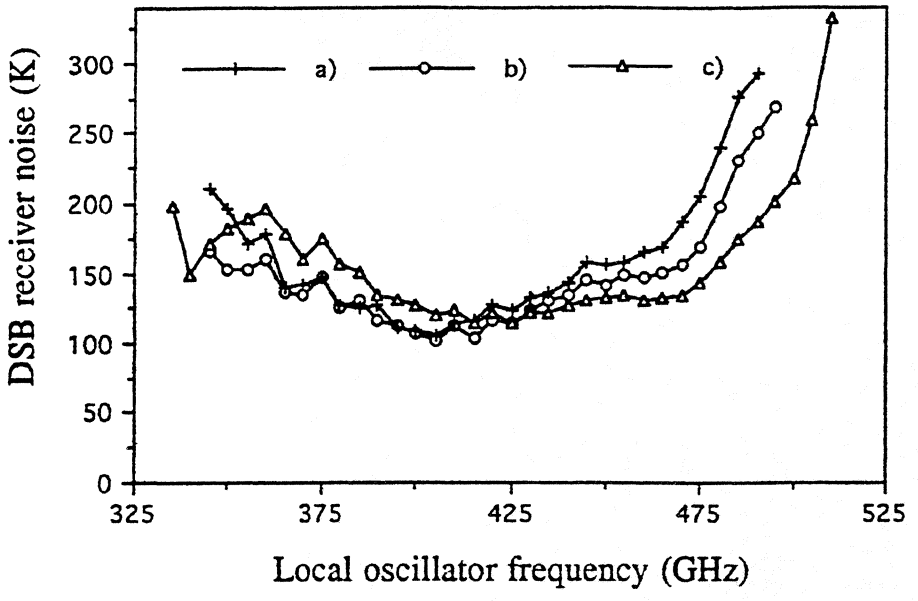

Figure 4: The DSB receiver noise is plotted as a function of LO frequency for a receiver with a mixer using SIS junctions of different sizes: a) 0.65 μm^2, b) 0.58 μm^2, c) 0.5 μm^2.

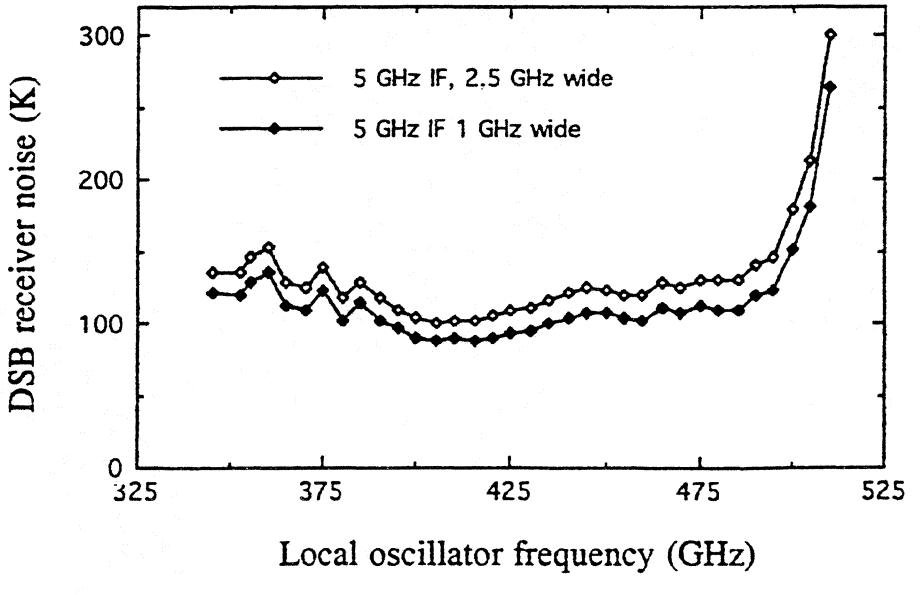

Figure 5: The DSB receiver noise as a function of LO frequency for two IF bandwidths.

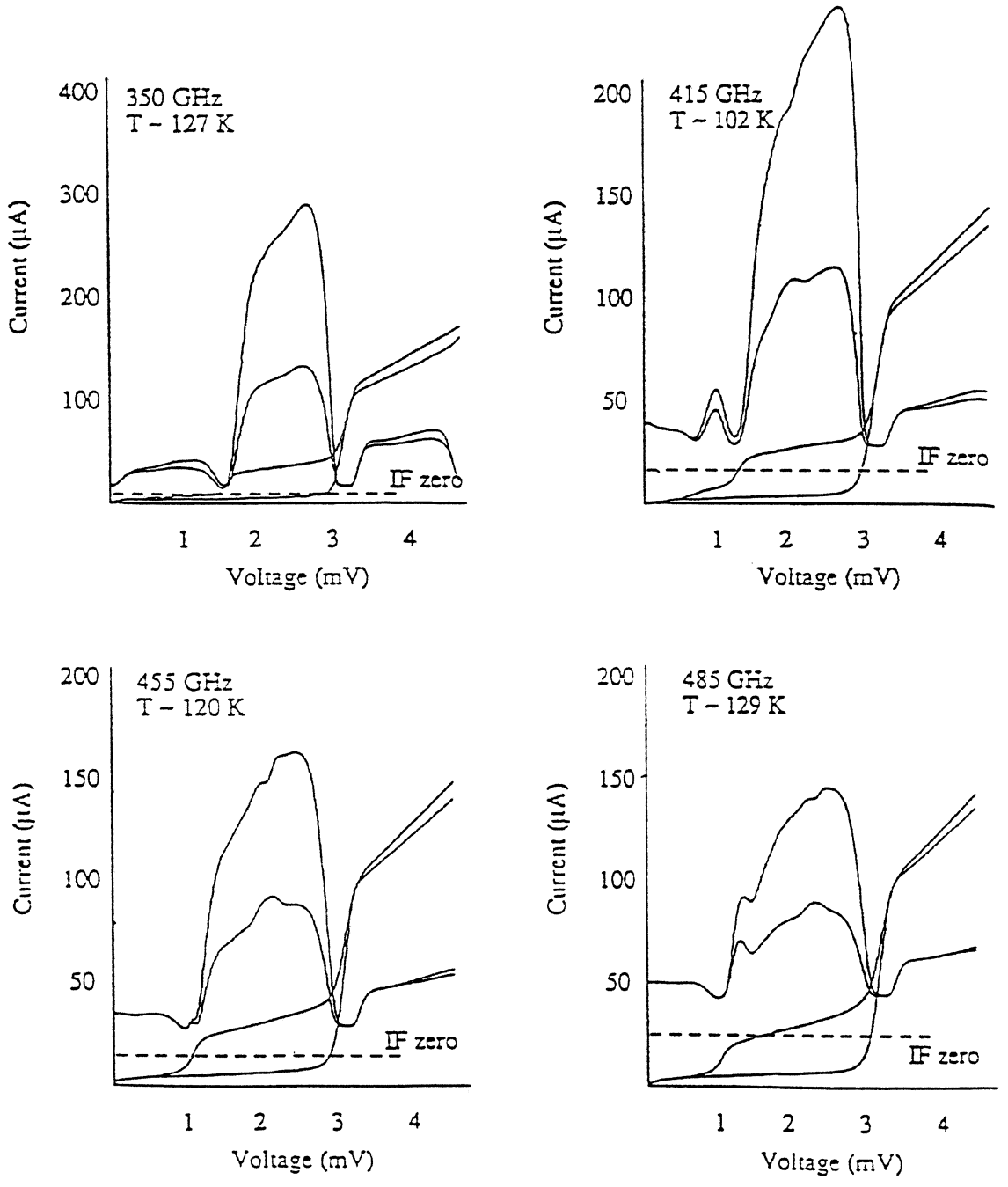

Figure 6: Current-voltage curves, pumped and unpumped, are given as a function of LO frequency. Also shown is the receiver's response to hot, 295 K, and cold, 77 K, input loads.

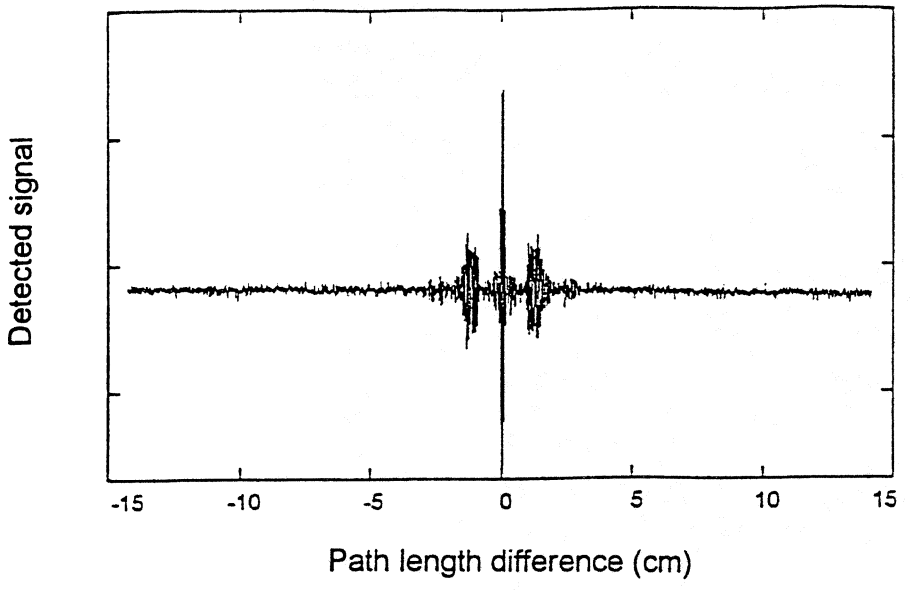

Figure 7a: FTS output interferogram of the SSB mixer receiver.

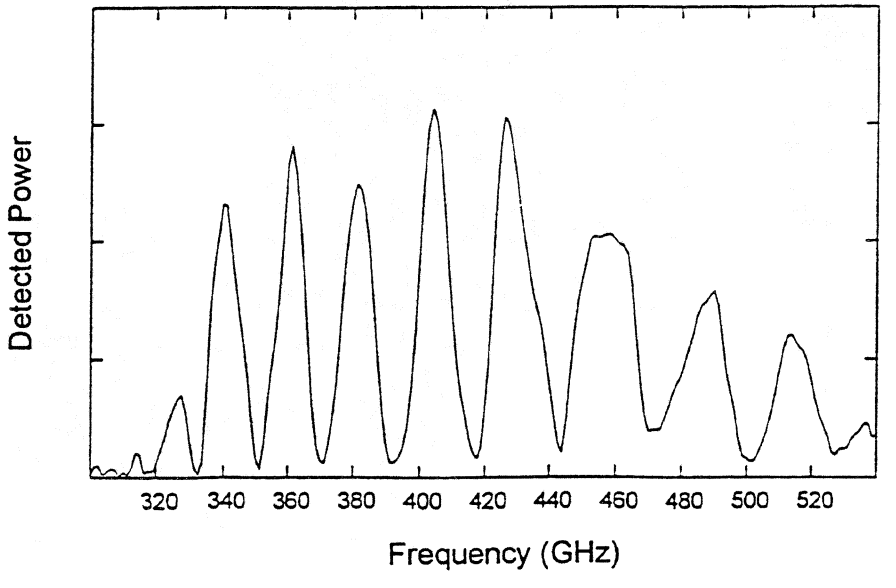

Figure 7b: Corresponding receiver response as a function of signal frequency.

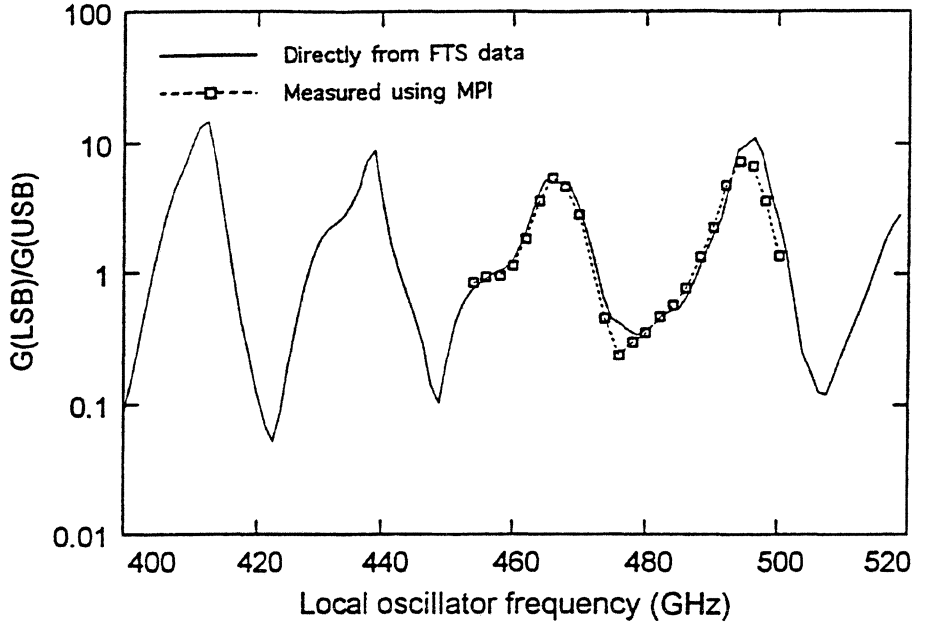

Figure 8: LSB to USB gain ratio as a function of LO frequency for the SSB receiver.

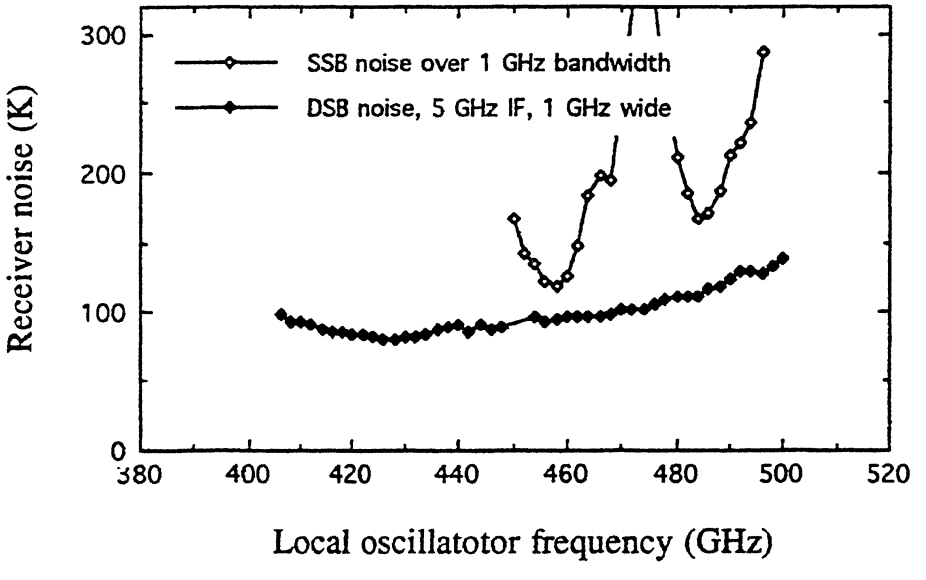

Figure 9: SSB and DSB receiver noise, calculated from Y-factor measurements, as a function of LO frequency from SSB and DSB mixers using the same SIS junction.